

# INFLUENCE OF SELF-COMPLEMENTARY HYDROGEN BONDING ON SOLUTION PROPERTIES OF CELLULOSE ACETATE PHTHALATE IN SOLVENT/NON-SOLVENT MIXTURES

ADINA-MARIA DOBOS, MIHAELA-DORINA ONOFREI, IULIANA STOICA,  
NICULAE OLARU, LILIANA OLARU and SILVIA IOAN

*Romanian Academy, "Petru Poni" Institute of Macromolecular Chemistry, Iasi, Romania*

Received September 21, 2012

The transition from the unentangled regime to the entangled one at higher concentration and the existence of hydrogen bonding were analyzed by dynamic viscosity. In addition, morphological properties of cellulose acetate phthalate (CAP) in solvent/non-solvent mixtures of 2-methoxyethanol/water were studied. The increase of water content contributed significantly to hydrogen bonding with cellulose acetate phthalate, generating the entanglement process, along with other types of interactions. Our research demonstrated that CAP easily dissociate in a relatively low polar solvent, such as 2-methoxyethanol, leading to strong intermolecular interaction with the addition of water, ascertaining the influence of hydrogen bonding on the thermodynamic properties. This study is significant for using cellulose acetate phthalate in different domains.

**Keywords:** cellulose acetate phthalate, solution properties, entanglement process

## INTRODUCTION

The increasing need for materials to be used in new applications requires polymers with diverse architectures, which would induce specific properties.<sup>1,2</sup> Among such materials, cellulose acetate phthalate (CAP) has been used for several decades as a pharmaceutical excipient; enteric coatings based on CAP are resistant to acidic gastric fluids, but easily soluble in the mildly basic medium of the intestine. The pH sensitive solubility of CAP is mainly determined (as other properties of this mixed ester) by the degree of substitution (DS), namely the average number of substituent groups bound to an anhydroglucose unit, as well as by the molar ratio (acetyl and phthaloyl groups).

These two structural characteristics of the polymer are dependent on the method employed for its synthesis. Recently, its potential to inhibit infections by human immunodeficiency virus type 1, several herpes viruses and other sexually transmitted disease pathogens has been investigated *in vitro*.<sup>3,4</sup> Also, CAP has been used for enteric film coating of tablets and capsules, which confirms its well-established safety for human use. In addition, intense research efforts have been focused on the design and fabrication

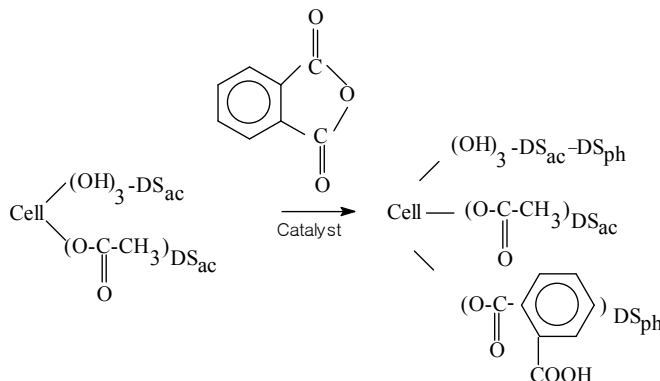
of nano-fibers or metal nano-particles in polymers, due to their novel electronic, optical, magnetic and chemical properties.<sup>5,6</sup>

As known, solvents contribute essentially to the modification of the solution behavior (association, complex, micelle, and core-shell structure of the polymer chains), and also to the processes that determine the membrane morphology of cellulose derivatives. Most of the parameters that play an important role in the formation of cellulose acetate (CA) membranes have been studied in detail. Of these variables, one should mention the nature of cellulose and the substitution degree of CA, the nature of the casting solvent mixtures, their composition and temperature.<sup>5-8</sup>

Extensive studies have been conducted on the effect of the solvents used on the morphology and performance of CAP or CAP blends with various polymers in different applications, such as ultrafiltration membranes, reverse-osmosis membranes, gas-separation membranes, and pervaporation membranes. The addition of a second solvent to the casting solution increases the permeation flux of a membrane or improves the performance of nano-fibers.<sup>9</sup>

Literature data<sup>10,11</sup> reveal that the structures, boiling point, content of solvent mixture, and intrinsic viscosity may affect performance in some applications. Moreover, the electrospinning process of polymers in solvent mixtures employs

an electrostatic potential to form fibers with different diameters. These fibrous mats with high specific surface area and nano-degree of porosity lend themselves to a wide range of applications.



Scheme 1: Obtaining of cellulose acetate phthalate from cellulose acetate (substitution degree = 1.93), in the presence of phthalic anhydride<sup>13</sup>

In some previous papers, the synthesis of cellulose acetate<sup>12</sup> and cellulose acetate phthalate,<sup>13</sup> as well as some properties of cellulose acetate phthalate<sup>14</sup> were studied.

In the present work, the effect of 2-methoxyethanol(2-Me)/water(W) mixtures on the CAP solution properties, especially in the semi-dilute domain, is investigated for evidencing the unentangled–entangled transition. In addition, the study demonstrates that the existence of rheological/morphological relationships in CAP solutions leads to the formation of hydrogen bonding associations. The results will be used for optimizing the polymer solution properties in the future applications of cellulose acetate phthalate.

## EXPERIMENTAL

### Materials

Cellulose acetate with a 1.93 substitution degree was used for the synthesis of cellulose acetate phthalate. Cellulose acetate was phthaloylated with phthalic anhydride in acetic acid media using anhydrous sodium acetate and triethylamine as basic catalysts, according to Scheme 1.<sup>13</sup>

Phthaloylation of CA in acetic acid was performed at 70 °C for 4 h. The viscous solution of CAP thus obtained was diluted with an aqueous solution of 75 wt% acetic acid. The polymer was separated from this solution by precipitation into cold water, filtered on a Büchner funnel, and purified by washing with distilled water until the washing liquid was free of acidity. Finally, the product was air-dried. The degrees of CA

acetylation (DSac) (determined by the usual saponification method) and of CAP phthaloylation (DSph) (determined by titration of carboxyl groups with sodium hydroxide) were of 1.73 and 0.7, respectively.<sup>13</sup>

### Measurements

Viscosity measurements were carried out in 2-methoxyethanol/water mixtures, at 25 °C ( $\pm 0.01$  °C), on a Schott AVS 350 computerized apparatus provided with an Ubbelohde suspended-level viscometer. The composition range of the mixed solvents was selected as a function of cellulose acetate phthalate solubility. Prior to the measurements, performed during a single day, the samples had been kept in solution for 5 h. The concentration domain was 0.6-1 g/dL. The kinetic energy corrections were negligible. The flow volume of the viscometer used exceeded 5 mL, making drainage errors unimportant. Flow times were obtained with an accuracy of approx. 0.035%, for different measurements in 2-methoxyethanol/water, at a given temperature. Intrinsic viscosities,  $[\eta]$ , were determined by Rao equations:<sup>15</sup>

$$\frac{1}{2(\eta_{rel}^{1/2} - 1)} = \frac{1}{[\eta]c} - \frac{(a-1)}{2.5} \quad (1)$$

where  $c$  is the concentration of polymer solution,  $a = 1/\Phi_m$ ,  $\Phi_m$  being the maximum volume fraction to which the particles can pack, expressed as  $\Phi_m = [\eta]/2.5 \cdot c_m$ .

The preferential adsorption coefficients,  $\lambda_1$ , were directly accessible from the experiments, through

interferometry (Zeiss interferometer) at 25 °C and dialysis equilibrium, according to equation (2):

$$\lambda_1 = \frac{(dn/dc)_\mu - (dn/dc)_u}{dn_0/d\phi_1} \quad (2)$$

where  $(dn/dc)_u$  and  $(dn/dc)_\mu$  are the refractive index increments of the polymer in 2-methoxyethanol/water solvent mixtures, before and after establishing dialysis equilibrium, respectively, and  $dn_0/d\phi_1$  is the variation of the refractive index increment of the solvent mixture as a function of 2-methoxyethanol volumetric composition.

Equilibrium dialysis experiments of cellulose acetate phthalate (3) in 2-methoxyethanol (1)/water (2) mixed solvents were carried out in a dialyser with a total volume of about 15 mL. Before use, the semipermeable cellophane membrane was conditioned in each of the solvent mixtures. Dialysis equilibrium was obtained within 6 h. The solvent systems were selected as a function of the substitution degrees of cellulose acetate phthalate, which determined the solubility in the different domains of solvent mixtures.

The refractive index of the 2-methoxyethanol/water mixed solvent was assessed on an Abbe refractometer at 25 °C to obtain the refractive index variation of mixtures with the volume fraction of solvent.

Rheological measurements of cellulose acetate phthalate in 100/0, 80/20 and 70/30% v/v 2-methoxyethanol (2-Me)/water (W) solvent mixtures were obtained with a Bohlin Instrument, by the cone and plate measuring system; the cone had an angle of 4° and a diameter of 40 mm. The rheological data were realized for the 3-15 g/dL concentration domain, at 25 °C.

The films used for atomic force microscopy (AFM) investigations were prepared from cellulose acetate phthalate solutions of 15 g/dL concentration, in 2-methoxyethanol/water solvent mixtures with different compositions. The polymer solutions were cast on glass plates and initially solidified by slow drying in a solvent-saturated atmosphere, and finally under vacuum, at 30 °C. The CAP membranes thus prepared were subjected to AFM analysis.

Atomic force microscopy (AFM) images were obtained on an SPM SOLVER Pro-M instrument. An NSG10 “Golden” Silicon probe tip with a 10 nm curvature radius and 255 kHz oscillation mean frequency was used to investigate membrane surface morphology. The apparatus was operated in the semi-contact mode, over a 20 x 20 μm<sup>2</sup> scan area, 256 x 256 scan point size images being thus obtained.

## RESULTS AND DISCUSSION

### Conformational properties of cellulose acetate phthalate in solution

The influence of solvent mixtures on the conformational properties of cellulose acetate phthalate in dilute solution was estimated by coil

density,  $\rho$ , of the polymer chains in solution and intrinsic viscosity in a perturbed and unperturbed state, as follows:<sup>16-18</sup>

$$\rho = \frac{c}{\eta_{sp}} \left( 1.25 + 0.5 \sqrt{56.4 \eta_{sp} + 6.25} \right) \quad (3)$$

or

$$\rho = \frac{c^*}{0.77^3} \left\{ 1 + \frac{[\eta] - [\eta]_\theta}{[\eta]_\theta} \left[ 1 - \exp\left(-\frac{c}{c^*}\right) \right] \right\} \quad (4)$$

Here  $\eta_{sp} = t/t_0 - 1$  is specific viscosity,  $t$  and  $t_0$  are the flow times of the polymer solution and of the solvent, respectively,  $c^*$  is the critical concentration at which the polymer coils begin to overlap, defined by equation (5), and  $[\eta]$  is the intrinsic viscosity in an unperturbed state, defined by equation (6):

$$c^* = \frac{0.77}{[\eta]} \quad (5)$$

$$[\eta]_\theta = \frac{[\eta] \left[ 1 - \exp\left(-\frac{c}{c^*}\right) \right]}{\frac{0.77^3 \rho}{c^*} - \exp\left(-\frac{c}{c^*}\right)} \quad (6)$$

Figure 1 shows the coil density dependence on concentration, for CAP, in 2-methoxyethanol and 2-methoxyethanol/water at 80/20, 75/25, 70/30 and 50/50 v/v, in the dilute range, as well as for a large concentration domain. The small plot in Figure 1 corresponds to the experimental data obtained in a dilute solution. Polymer coil density increases with increasing polymer concentration while, above a critical concentration in the semi-dilute domain,  $c^+$ , coil density remains constant. Thus, density at  $c^+$  represents the density in the unperturbed state.

The modification of coil density is reflected by the variation of the radius of gyration with concentration, evaluated by equation (7).

$$R_g^3 = \frac{3M[\eta]}{3\phi \left\{ 1 + \frac{[\eta] - [\eta]_\theta}{[\eta]_\theta} \left[ 1 - \exp\left(-\frac{c}{c^*}\right) \right] \right\}} \quad (7)$$

The dependences between dimensions and concentration are illustrated in Figure 2, where the small plot corresponds to the experimental data for the dilute solution. The radii of gyration decrease with increasing concentration while, at the critical concentration  $c^+$ , they are considered to shrink to their unperturbed dimensions. Thus, the radius of gyration at  $c \geq c^+$  corresponds to the radius of gyration in the unperturbed state. The critical concentrations,  $c^+$ , are approximated by  $c^+ \cong 8c^*$ .

The thermodynamic parameters represented by the intrinsic viscosities,  $([\eta])$ , the radii of gyration in perturbed,  $R_{g,c=0}$ , and unperturbed states,  $R_{g,c=\infty}$  (according to Figure 2), and the critical concentrations that delimited the dilute/semi-dilute domain ( $c^*$ ), semi-dilute unentangled/semi-dilute entangled domain ( $c^{**}$ ) and semi-dilute/concentrated domain ( $c^{***} = c^*$  ( $R_{g,c=0}/R_{g,c=\infty}$ )<sup>8</sup>), are presented in Table 1.

Table 1  
Critical concentrations, gyration radius in perturbed and unperturbed state and intrinsic viscosity for CAP in 2-Me/W (% v/v)

2-Me/W	$c^*$ (g/dL)	$c^{**}$ (g/dL)	$c^+$ (g/dL)	$c^{***}$ (g/dL)	$R_{g,c=0} \times 10^8$ (cm)	$R_{g,c=\infty} \times 10^8$ (cm)	$[\eta]$ (dL/g)
100/0	1.25	7.40	9.98	19.79	106.00	75.05	0.617
80/20	1.26	7.93	10.07	20.35	105.81	74.72	0.612
75/25	1.26	-	10.07	21.29	105.78	74.28	0.611
70/30	1.37	9.80	10.93	21.75	104.93	74.27	0.563

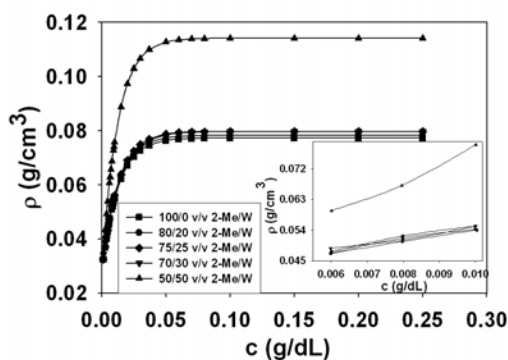


Figure 1: Variation of coil density with concentration of cellulose acetate phthalate, in 2-Me/W solvent mixtures, at 25 °C. The small plot corresponds to experimental data in dilute solution

The values obtained for the unperturbed dimension parameters show the influence of solvent mixtures. The perturbed and unperturbed dimensions of the cellulose acetate phthalate decrease with increasing water content. Thus, such decreases might be induced by the modification of the solvation power of the solvent mixtures.

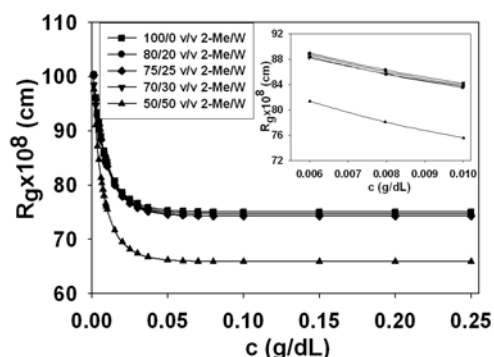


Figure 2: Variation of gyration radius with concentration of cellulose acetate phthalate, in 2-Me/W solvent mixtures, at 25 °C. The small plot corresponds to experimental data in dilute solution

### Preferential adsorption

Table 2 illustrates the variation of the preferential adsorption coefficient,  $\lambda_1$ , with the 2-methoxyethanol content,  $\phi_1$ , for CAP, in the 2-methoxyethanol (1)/water (2) binary mixture, determined experimentally from refractive index increments, both before,  $(dn/dc)_u$ , and after,  $(dn/dc)_\mu$ , establishing dialysis equilibrium from equation (2), considering refractive index increment of solvent mixture  $(dn_0/d\phi_1)$  of 0.072.

The values of  $dn_0/d\phi_1$  in range of 0-100% solvent mixtures were obtained from the derivation of the linear dependences expressed by equation (8).

$$n_0 = 1.330 + 0.072\phi_1 \quad (8)$$

where  $n_0$  is the refractive index of the mixed solvents. According to the intrinsic viscosity values, 2-methoxyethanol is a good solvent for CAP and the addition of water decreases the quality of the solvent mixtures in 0-0.30 volume fractions of the water. In addition, 2-methoxyethanol is preferentially adsorbed ( $\lambda_1$  shows positive values) within the mentioned domains and both solvents tend to minimize the preferential adsorption at the limit values of  $\phi_1$ . Consequently, from preferential adsorption data, two distinct ranges of water composition can be distinguished, where the solvent mixture has

different interactive properties. Therefore, the polymer chains have the tendency to surround themselves with the most thermodynamically

efficient solvent, at a given composition of the solvent mixture.

Table 2  
Specific refractive index increments before and after dialysis equilibrium for CAP in 2-methoxyethanol/water and refractive index increment of solvent mixture,  $(dn_0/d\phi_1)$

$\phi_1$	$(dn/dc)_u$	$(dn/dc)_e$	$(dn_0/d\phi_1)$	$\lambda_1$
0.80	0.100	0.133	0.072	0.460
0.75	0.091	0.140	0.072	0.685
0.70	0.087	0.125	0.072	0.526

### Rheological investigation

The modification of the cellulose acetate phthalate dynamic viscosity for different compositions of 2-methoxyethanol/water was analyzed. The study focused only on shear rheological measurements as a means to determine the critical concentrations, where the transition from the semi-dilute unentangled to the semi-dilute entangled regimes occurs. Figure 3 shows the influence of the 2-Me/W solvent mixtures composition on the dynamic viscosities.

The dynamic viscosity presents a Newtonian behavior for all compositions of the solvent mixtures and increases with decreasing the water content. Considering the dynamic viscosity in the Newtonian regime at a low shear rate, equivalent with zero shear rate viscosity, specific viscosity  $\eta_{sp}$  was determined by equation (9):

$$\eta_{sp} = \frac{\eta_0 - \eta_s}{\eta_s} \quad (9)$$

where  $\eta_0$  is the zero shear rate viscosity of the solution and  $\eta_s$  is the solvent viscosity.

The entanglement concentration,  $c^{**}$ , which is defined as the transition from the semi-dilute unentangled regime to the semi-dilute entangled one, was measured using the change in slope at

$$\log \eta_{sp} = 1.603 + 1.215 \cdot (c \cdot [\eta]) + 5.207 \cdot (c \cdot [\eta])^2 + 1.093 \cdot (c \cdot [\eta])^3 \quad \text{for 100/0\% v/v} \quad (10)$$

$$\log \eta_{sp} = 1.673 + 1.205 \cdot (c \cdot [\eta]) + 4.781 \cdot (c \cdot [\eta])^2 + 1.124 \cdot (c \cdot [\eta])^3 \quad \text{for 80/20\% v/v} \quad (11)$$

$$\log \eta_{sp} = 2.759 + 1.379 \cdot (c \cdot [\eta]) + 4.045 \cdot (c \cdot [\eta])^2 + 1.190 \cdot (c \cdot [\eta])^3 \quad \text{for 70/30\% v/v} \quad (12)$$

In this context, it may be observed that decreasing the solvent mixture quality leads to higher values for  $\eta_{sp}$  and higher values for  $c^{**}$  concentrations. In addition, the  $\eta_{sp}$  power law

the onset of the entangled regime.<sup>19</sup> It is known that for non-associating polymers  $\eta_{sp} \propto c^{**1.25}$  in the semi-dilute unentangled regime,  $\eta_{sp} \propto c^{**4.8}$  in the semi-dilute entangled regime, if the polymer is in a theta solvent, and  $\eta_{sp} \propto c^{**3.7}$  in the semi-dilute entangled regime, if the polymer is in a good solvent.<sup>20</sup>

Figure 4 shows the dependence of the specific viscosity for the CAP solutions in 2Me/W solvent mixtures at 25 °C as a function of a dimensionless parameter,  $c \cdot [\eta]$ , known as the coil overlap parameter, which provides an index of the total volume occupied by the polymer.

A slope modification in these dependences occurs at critical concentrations,  $c^{**}$ , and separates the semi-dilute unentangled domain from the semi-dilute entangled one. As a function of the solvent mixture composition, these concentrations have the following values: 8.69, 9.55 and 10.00 g/dl for 100/0, 80/20 and 70/30% v/v 2-Me/W, respectively. In addition, the dependences between specific viscosity and concentration from Figure 4 can be expressed by the following equations:

exponent in the semi-dilute entangled regime increases from 4.5 to 5.5 for 100/0-70/30% v/v solvent mixture compositions. This indicates that, on the one hand, increasing the water content leads to a decrease in the quality of the solvent mixtures, and, on the other hand, increasing

polarity by adding water leads to an increase in the number of intermolecular polymer associations.

On the contrary, according to Table 1 and Figure 4, in the dilute and in the semi-dilute unentangled domain,  $\eta_{sp}$  increases as the 2-Me content increases, suggesting that 2-Me is a better solvent for CAP than 80/20 v/v 2-Me/W or 70/30 v/v 2-Me/W.

These evaluations show that  $\eta_{sp}$  increases with solvent quality for the dilute or semi-dilute unentangled chains, due to a stronger apparent

repulsive force among chain segments, and  $\eta_{sp}$  decreases with increasing solvent quality for the chains in the entangled regime. This phenomenon has been described in literature by a two-parameter scaling relationship for the polymers in the entangled regime,<sup>20</sup> and the increase in  $\eta_{sp}$  with decreasing solvent quality in the entangled regime has been reported to be due to a greater number of entanglement couplings in the poor solvent, which result from stronger attractive forces between the chain segments.<sup>19,21</sup>

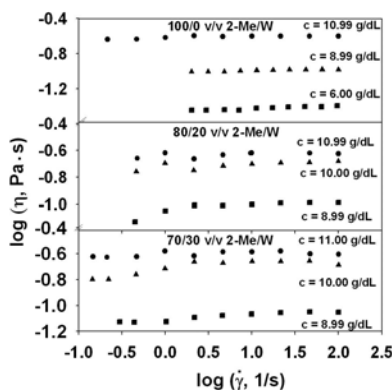


Figure 3: Log-log plots of dynamic viscosity versus shear rate for CAP with different compositions of 2-Me/W solvent mixtures and different concentrations

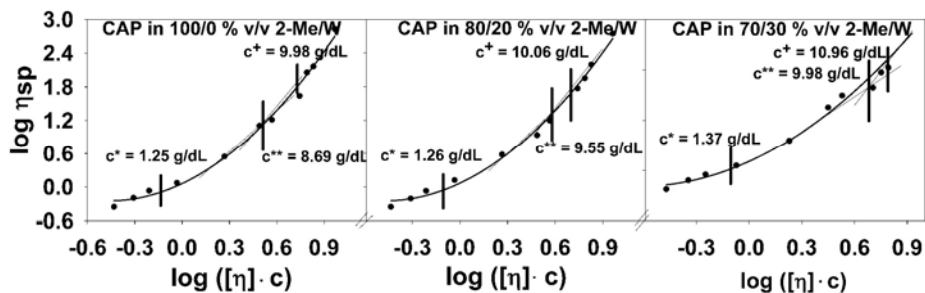


Figure 4:  $\eta_{sp}$  dependence on  $c \cdot [\eta]$  for CAP in 2-methoxyethanol/water solvent mixtures at different compositions

In addition, one can remark that the increase of the water content over the 0.70 volume fraction displays significant hydrogen bonding with cellulose acetate phthalate, generating the entanglement process among other types of interactions generated by carboxyl groups. Thus, our research demonstrates that CAP, which contains carboxyl and hydroxyl groups, is able to develop hydrogen bonding, easily dissociates in a relatively low polarity solvent, such as 2-Me, and leads to strong intermolecular interaction with the

addition of higher polarity water, showing the influence of hydrogen bonding on the thermodynamic properties. Therefore, the transition from the semi-dilute unentangled regime to the semi-dilute entangled one is determined by solvent polarity. The concentration corresponding to this transition increases from 8.69 g/dL in 100/0% v/v 2-Me/W to 9.98 g/dL in 70/30% v/v 2-Me/W. A preliminary study established an optimal concentration of around 30 g/dL for obtaining nano-fibers. According to

Table 1, this concentration is located at the upper limit of the semi-dilute–concentrated domain. Olaru *et. al.*<sup>22</sup> have shown that the solvent employed plays an important role in the electrospinning process. In this context, it has been found that the optimal concentration of CAP for obtaining nano-fibers is: 35%, 25% and 12.5% in 2-Me, 50/42.5/7.5 v/v/v 2-Me/acetone (Ac)/W, in 85/15 v/v acetone/water, respectively. These concentrations correspond to the entangled domain and decrease with the decrease of solvent mixtures' quality.

### Morphological properties

It has been reported that the chain shape of a polymer in solution could affect the morphology of the polymer in bulk.<sup>10,23</sup> The cellulose acetate phthalate membranes used in atomic force microscopy examination were prepared from 2-methoxyethanol/water, solvent/non-solvent mixtures. Thus, for the studied CAP, intrinsic viscosity (Table 1) and the preferential adsorption coefficient (Table 2) *versus* water content show a modification of the chain conformation in the dilute solution and over the whole composition range of the solvent mixtures.

2D and 3D AFM images were used to examine the film surfaces and to measure their surface topography. All images presented in Figure 5 were recorded under ambient conditions, over 20 x 20  $\mu\text{m}^2$  scan areas, to provide morphological details.

Each micrograph shows that the membrane surfaces have pores and nodules with different characteristics, as may be noted in Table 3, which includes the pore number (No.), diameter (d), depth (dp), perimeter (p) and area (A), and surface roughness parameters, including average roughness (Sa), root-mean-square roughness (Sq), nodule height from the height profile (nhp), and average height from the histogram (Ha).

According to our data, the water content in the casting solutions favors the occurrence of higher roughness, more visible for intermediary compositions of the solvent mixtures, which corresponds to the maximum of preferential adsorption,  $\lambda_1$ . In addition, for extreme water contents, the root-mean-square roughness of the surface (rms) decreases, the phenomenon being more intense at higher water contents. This conclusion is supported by Figure 6, which presents the profiles and histograms of AFM images.

Table 3  
Pore characteristics of membranes prepared from cellulose acetate phthalate solutions in different 2-Me/W solvent mixtures (% v/v)

Solvent mixtures	Pore characteristics					Surface roughness			
	No.	d ( $\mu\text{m}$ )	dp (nm)	p ( $\mu\text{m}$ )	A ( $\mu\text{m}^2$ )	Sa (nm)	Sq (nm)	nhp (nm)	Ha (nm)
100/0	9	4.1	12.5	12.7	13.0	2.0	2.9	17.8	8.1
80/20	18	1.8	13.0	5.8	2.6	3.4	4.3	26.3	17.8
70/30	23	0.6	7.2	1.7	0.2	1.6	2.5	23.0	9.9

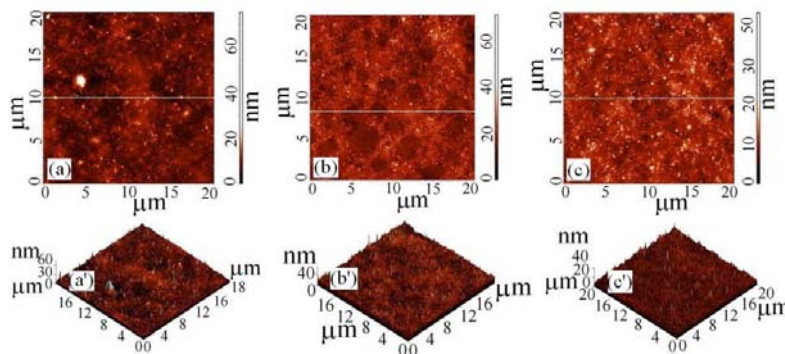


Figure 5: 2D (a, b, c) and 3D (a', b', c') AFM images of CAP films obtained in different 2-methoxyethanol/water solvent mixtures: 100/0, 80/20, and respectively, 70/30% v/v

On the other hand, AFM images show that, the number of pores increases when the water content is higher, while their characteristics (diameter, depth, perimeter and area) decrease. In fact, further quantitative information on pore characteristics can be obtained by analyzing the images. In Figure 7, pore number distributions

attending to pore size, as obtained from the AFM image analysis,<sup>24,25</sup> are presented for CAP films, allowing the evaluation of diameter average values from Table 3.

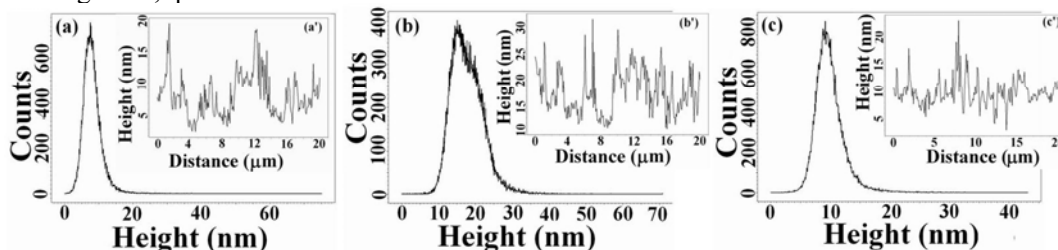


Figure 6: Histogram and surface profile (small plot) taken along a line from 2D AFM images of cellulose acetate phthalate films obtained in different 2-methoxyethanol/water solvent mixtures: (a, a') 100/0% v/v; (b, b') 80/20% v/v; (c, c') 70/30% v/v

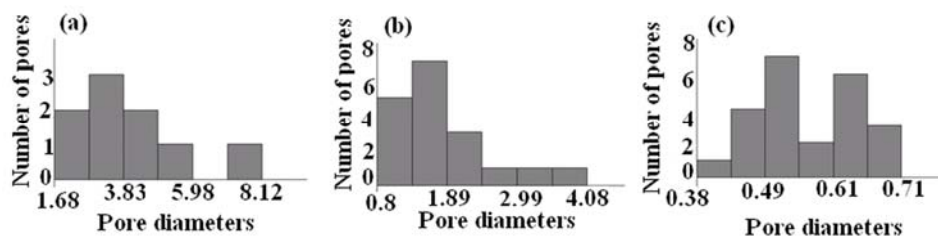


Figure 7: Pore number distribution attending to pore size as obtained from AFM image analysis

All investigations indicate that the membrane properties depend not only on the substitution degrees of the cellulose acetate phthalate, but also on the composition of the solvent mixtures. In particular, it was found out that decreasing solvation power, observed from viscometric studies in dilute solution, favors an increase in pore number.

## CONCLUSION

The modification of intrinsic viscosity and of the preferential adsorption coefficients of cellulose acetate phthalate in 2-methoxyethanol/water solvent/non-solvent mixtures has been investigated. The solutions are characterized by the existence of association phenomena over the 0.30 volume fraction of the water content. The viscometric measurements from the solubility domain allowed the evaluation of unperturbed and perturbed viscosity, dimensions, density, as well as critical concentra-

tions, which separate the dilute and semi-dilute/concentrated domains.

The rheological study has focused on shear rheological measurements as a means to determine the critical concentration, where the transition from the semi-dilute unentangled regime to the semi-dilute entangled one occurs. One can observe that in the dilute and in the semi-dilute unentangled domains, viscosity increases as the non-solvent composition decreases due to a stronger apparent repulsive force between chain segments, while in the entangled regime, decreasing the solvent mixture quality leads to higher values for viscosity and higher values for entanglement concentration – defined as the transition from the semi-dilute unentangled regime to the semi-dilute entangled one. Thus, the research demonstrates that cellulose acetate phthalate, which contains carboxylic groups, able to develop hydrogen bonding, easily dissociates in a relatively low polarity solvent, and leads to



strong intermolecular interaction through the addition of water with higher polarity, showing the influence of hydrogen bonding on the thermodynamic properties.

According to AFM data, the water content in the casting solutions favored the occurrence of roughness, more visible for intermediary compositions of the mixed solvents, which corresponds to better preferential adsorption of 2-methoxyethanol from the solvent mixtures. For extreme water compositions, lower average roughness values and root-mean-square roughness values appear, the phenomenon being more intense at higher water contents. On the other hand, increasing the water content in casting solutions determines the modification of the pore number and pore characteristics in AFM images, so that at high water content, the pore number is maximum, while the area, perimeter, and diameter are minimum. This changing trend in morphology is due to the modification of the polymer chain conformation in solution.

These studies assure the main properties necessary for expanding the application areas of cellulose acetate phthalate, involving the knowledge of conformational properties, preferential adsorption coefficients and the entanglement process – known as depending on the interaction parameters of the polymer/solvent/non-solvent systems.

## REFERENCES

- <sup>1</sup> K. J. Edgar, C. M. Buchanan, J. S. Debenham, P. A. Rundquist, B. D. Seiler, M. Shelton and D. Tindall, *Prog. Polym. Sci.*, **26**, 1605 (2001).
- <sup>2</sup> A. Shanbhag, B. Barclay, J. Koziara and P. Shivanand, *Cellulose*, **14**, 65 (2007).
- <sup>3</sup> A. Stone, *Microbicides*, **1**, 977 (2002).
- <sup>4</sup> K. H. Manson, M. S. Wyand, C. Miller and A. R. Neurath, *Antimicrob. Agents Chemother.*, **44**, 3199 (2000).
- <sup>5</sup> R. E. Southward and D. W. Thompson, *Mat. Des.*, **22**, 565 (2001).
- <sup>6</sup> Y. Yuan, J. H. Fendler and I. Cabasso, *Chem. Mat.*, **4**, 312 (1992).
- <sup>7</sup> I. Shim, C. S. Wun, W. T. Noh, J. Y. Kwon, D. Y. Cho Chae and K. S. Kim, *Bull. Korean Chem. Soc.*, **22**, 772 (2001).
- <sup>8</sup> I. W. Shim, J. Y. Kim, D. Y. Kim and S. Choi, *React. Funct. Polym.*, **43**, 71 (2000).
- <sup>9</sup> S. G. Kim, Y. L. Kim, H. G. Yun, G. T. Lim and K. H. Lee, *J. Appl. Polym. Sci.*, **88**, 2884 (2003).
- <sup>10</sup> J. W. Qian, Q. F. An, L. N. Wang, L. Zhang and L. Shen, *J. Appl. Polym. Sci.*, **97**, 1891 (2005).
- <sup>11</sup> D. M. Wang, T. T. Wu, F. C. Lin, J. Y. Hou and J. Y. Lai, *J. Membr. Sci.*, **169**, 39 (2000).
- <sup>12</sup> N. Olaru and L. Olaru, *J. Appl. Polym. Sci.*, **94**, 1965 (2004).
- <sup>13</sup> N. Olaru and L. Olaru, *Iran. Polym. J.*, **14**, 1058 (2005).
- <sup>14</sup> A. M. Necula, S. Dunca, I. Stoica, N. Olaru, L. Olaru and S. Ioan, *Int. J. Polym. Anal. Character.*, **15**, 341 (2010).
- <sup>15</sup> M. V. S. Rao, *Polymer*, **34**, 592 (1993).
- <sup>16</sup> J. W. Qian and A. Rudin, *Eur. Polym. J.*, **28**, 733 (1992).
- <sup>17</sup> J. W. Qian and A. Rudin, *Eur. Polym. J.*, **28**, 725 (1992).
- <sup>18</sup> J. W. Qian, M. Wang, D. L. Han and R. S. Cheng, *Eur. Polym. J.*, **37**, 1403 (2001).
- <sup>19</sup> M. G. McKee, C. L. Elkins and T. E. Long, *Polymer*, **45**, 8705 (2004).
- <sup>20</sup> R. H. Colby and M. Rubinstein, *Macromolecules*, **23**, 2753 (1990).
- <sup>21</sup> Y. Isono and M. Nagawasa, *Macromolecules*, **13**, 862 (1980).
- <sup>22</sup> N. Olaru and L. Olaru, *Ind. Eng. Chem. Res.*, **49**, 1953 (2010).
- <sup>23</sup> D. Huangm, Y. Yang, G. Zhuang and B. Li, *Macromolecules*, **33**, 461 (2000).
- <sup>24</sup> M. J. Joralemon, K. S. Murthy, E. E. Remsen, M. L. Becker and K. L. Wooley, *Biomacromolecules*, **5**, 903 (2004).
- <sup>25</sup> N. A. Ochoa, P. Prádanos, L. Palacio, C. Pagliero, J. Marchese and A. Hernández, *J. Membr. Sci.*, **187**, 227 (2001).